CLINICAL AND EXPERIMENTAL
OPTOMETRY

ORIGINAL PAPER

# Applications of high-speed videokeratoscopy

*Clin Exp Optom* 2005; 88: 4: 223–231

**D Robert Iskander** PhD
**Michael J Collins** PhD
School of Optometry, Queensland University of Technology, Brisbane, Australia

Submitted: 17 February 2005
Revised 18 April 2005
Accepted for publication: 10 May 2005

High-speed videokeratoscopy is an emerging technology that has the potential to provide new information on dynamic changes of corneal topography and tear film behaviour. We have developed a high-speed videokeratoscope that has the ability to acquire data at the rate of 50 Hz. Two major applications of the technology are considered in this paper. First, the analysis of tear film stability in the inter-blink interval is evaluated and techniques for estimating the tear film build-up and break-up times are considered. The second application involves the study of the dynamic response of the corneal anterior surface to mechanical forces exerted by the eyelids during horizontal eye movements in downward gaze. The limitations and potential opportunities for the use of this new technology are discussed.

Key words: corneal topography, eyelids, tear film, videokeratoscope

Computerised videokeratoscopy is the current standard for measuring corneal topography.[1] Modern videokeratoscopes provide an accurate representation of the anterior corneal surface to allow assessment of corneal irregularities in keratoconus,[2] aid clinicians in contact lens fitting[3] and provide the means for evaluating the corneal contribution to optical aberrations of the whole eye.[4]

Most videokeratoscopes have the ability to acquire one videokeratograph at a time and allow the accumulation of a number of images before saving to computer memory is required. One videokeratoscope is able to register a sequence of several images at one-second intervals.[5] Another instrument continues acquiring topographical maps in real time and automatically scores the measurements according to criteria including best centring, focusing and least eye movements. In this way, the best measurements are retained.[6] At present there are no commercially available instruments that acquire corneal topography in a truly continuous dynamic manner.

As current videokeratoscopes acquire the image of a target reflected from the anterior surface of the eye, videokeratoscopic data represent the topography of the tear film covering the corneal surface. The tear film is constantly changing and undergoes reformation immediately after a blink, then exhibits a certain period of stability and finally undergoes break-up, provided the eye is left open for a sufficiently long period.[7] The first and last phases are often termed the tear build-up and break-up phases, respectively.

Recently, videokeratoscopes have been used to evaluate the temporal changes of the ocular surface. For example, Buehren and colleagues,[8] Nemeth, Erdelyi and Csakany[9] and Montes-Mico and associates[10,11] measured topography of the anterior cornea for several equidistant time intervals immediately after the blink. Such techniques provide additional information about the behaviour of the tear film that is unavailable when only a single measurement of topography is performed. However, they lacked the rigour of precise sampling and did not provide answers to tear film behaviour after a natural, unforced blink.

Nemeth and co-workers[12] were among the first who appreciated the importance of high speed videokeratoscopy. They adapted a commercially available videokeratoscope to acquire corneal elevation data at a sampling rate of 4 Hz for a period of 15 seconds. The raw videokeratoscopic images were stored in a computer

**Figure 1. Equipment set-up for high-speed (50 Hz) videokeratoscopy. VC: video card, VL: video link, DB: data base, HD: auxiliary hard drive.**

memory and processed later by the instrument's commercial software. With this system, Nemeth and co-workers[12] examined the dynamic changes in surface regularity and surface asymmetry indices (SRI and SAI)[13] and estimated the tear film build-up time by finding the minima of the estimated trends of SRI and SAI. To examine the tear film stability, several groups[14-16] have used an approach similar to that of Nemeth and co-workers[12] but with a sampling frequency of 1 Hz. They examined the behaviour of SRI and SAI immediately after a blink for a period of 10 seconds. Recently, Goto and colleagues[17] used changes in topographical power maps to estimate the tear film break-up time. They assumed that a time at which changes in corneal power are greater than 0.5 D corresponds to the time at which tear film break-up is observed.

Another application of high-speed videokeratoscopy deals with temporal changes of the corneal surface itself. It has been shown that the position of the eyelids can alter the corneal shape.[18,19] The changes in corneal shape can be significant, especially after reading[20] or after wearing certain types of contact lenses.[21] Buehren, Collins and Carney[20] have shown that these changes are directly related to the force applied by the eyelids during reading. In a following study,[22] the time of recovery of the corneal surface after reading is proportional to the period of time spent reading, this recovery process is non-linear. To understand the process of corneal recovery, it is of interest to evaluate these changes during and immediately after removal of the mechanical forces acting on the cornea. This task cannot be performed accurately with currently available videokeratoscopes.

Analysing the stability of the tear film during an inter-blink interval or the dynamics of corneal recovery are not the only functions envisaged for a high-speed videokeratoscopic system. Continuous measurement of corneal topography provides the opportunity to study such areas as the dynamics of corneal aberrations,[10] dynamics of ocular microfluctuations including dynamic cyclotorsion and dynamics of a contact lens on the eye. In addition, high-speed videokeratoscopy enables measurement of corneal elevation in subjects with nystagmus and those who are inattentive, and in infants or animals.

In this paper, we describe a new high-speed videokeratoscopic system that we have developed and we introduce novel methodologies for analysing dynamic corneal topographical data and tear film stability. In the process, we discuss the potential challenges and opportunities associated with such measurement systems. Two diverse applications of high speed videokeratoscopy are considered, including analysis of tear film stability and analysis of the dynamic recovery of the corneal surface after a short period of horizontal eye movements.

## HIGH SPEED VIDEOKERATOSCOPIC SYSTEM

We have developed a high-speed videokeratoscopic system that combines a commercially available instrument, the Medmont E300 unit (Medmont Pty Ltd, Melbourne, Australia) with an additional dynamic image acquisition system (Figure 1). An operator uses the first computer that runs the Medmont Studio and E300 Viewer software to align the instrument in a manner similar to traditional videokeratoscopes. The second computer uses Medmont Studio with DV2000 Digital Imaging software to acquire dynamic images at a rate of 50 Hz (that is, one frame every 20 milliseconds). This sampling rate was achieved by using the interlaced sub-frames of a CCD camera in the E300 unit. The computers were linked and shared one database, so there was no need for data transfer from one computer to the other. The hard drive of the first computer is used as an auxiliary back-up drive. Custom-written software processed the dynamically acquired images into a format recognised by the E300 Viewer software for post-processing of corneal elevation data.

An image sequence of 300 ms including a typical natural blink is shown in Figure 2. About 100 ms (the first six images) corresponds to the phase in which the eye is closing while in the remaining 200 ms the eye is opening. In most Placido-disc videokeratoscopes, the central or near central ring in the digital image needs to be clearly identified to properly calculate corneal topography. During recording of a blink, this condition may not always be guaranteed. For example, for the blink in Figure 2 the corneal topography cannot be evaluated in frames four to 10 (that is, seven frames, which equals 140 ms). Thus, for each recorded blink, several samples will be lost from the analysis (blink removal).

As with any high-speed filming, there are significant constraints on computer memory and data storage capacity. In our case, each raw grey-scale image requires about 440 KB. Assuming that the entire computer's RAM is not normally available for data acquisition, one can store roughly 40 seconds of recording for each GB of memory (RAM).

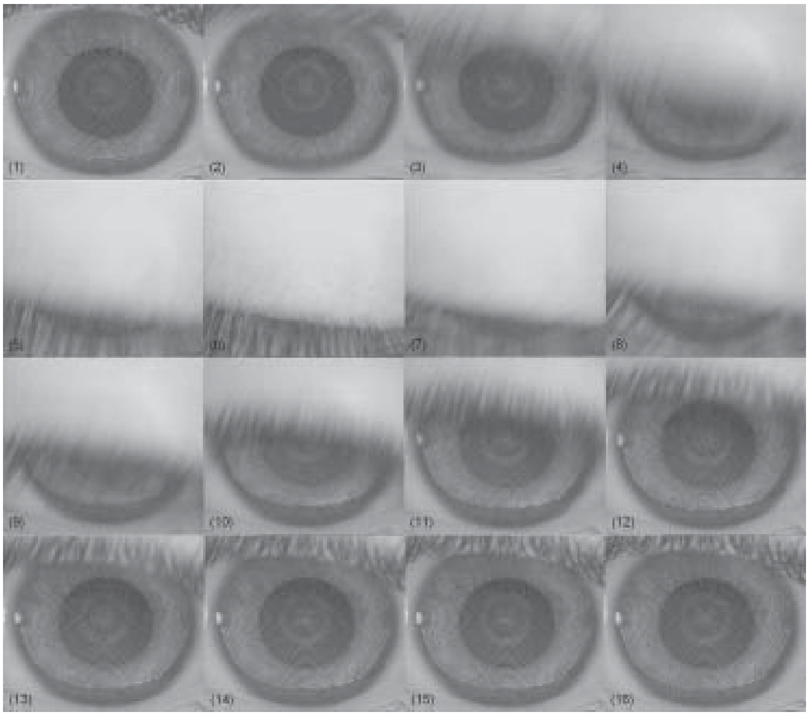

**Figure 2. A sequence of 16 consecutive raw images (300 ms) from the high speed videokeratoscope during a blink**

It is essential to store the acquired images to the memory buffer rather than directly to a file, so that instabilities in sampling (so-called jitter) are avoided.

## GENERAL ISSUES IN HIGH SPEED VIDEOKERATOSCOPIC DATA ANALYSIS

In previous studies,[12,14-17] the analysis of high-speed videokeratoscopic data amounted to the analysis of multiple measurements of corneal elevation taken at equidistant time intervals. In such an approach, each videokeratoscopic image is processed separately and no attempt is made to correlate the resulting topographical data in a series of measurements. This has its limitations as individual samples in the collection of measurements, whether a sequence of corneal topographies or a series of parameters derived from the topographical data such as SRI, SAI or a set of Zernike polynomial coefficients, cannot be related to each other without the assumption that the eye is stationary. In multiple videokeratoscopic measurements, ocular microfluctuations may need to be taken into account.[23]

Another important factor in both static and dynamic videokeratoscopic measurements is the level of noise. The measurement of noise in static acquisition of corneal topographical data has been well documented for artificial and real corneal surfaces,[24-26] however, little has been reported about the noise in dynamic data.

An instrument that is chosen for high-speed videokeratoscopy has two important features. First, the instrument needs an accurate range finder to determine the distance from the corneal apex to the imaging device. Second, it must provide accurate estimates of corneal surfaces that are taken off-axis. Our recent study,[27] with the Medmont E300 unit, in which multiple off-axis topographical maps have been combined to estimate the total limbus-to-limbus corneal elevation, shows that the instrument can accurately account for off-axis measurements. Given these provisions, we do not expect the level of measurement noise in high speed videokeratoscopy to be vastly different from that of a static measurement.

### Tracking ocular co-ordinates

A significant issue in high-speed videokeratoscopy is the movement of ocular co-ordinates during the extended measurement period. To estimate the variations in the position of the eye with respect to the instrument's axis, one can use surface correlation techniques[23] or estimate the limbal position in each frame of the recording. The latter can be performed automatically using our recently reported method of extracting limbal outlines from videokeratoscopic images,[28] provided that each image covers a good portion of the limbal outline. The extracted data corresponding to the corneal limbal outline is then fitted into a five-parameter elliptical model (that is, centre co-ordinates, major and minor axes, and rotation angle) using a method of least squares.

In Figure 3, we show examples of high-speed videokeratoscopic images for which we automatically estimated the limbal outlines. Frame 1 of Figure 2 is a typical example of an image acquired in an inter-blink interval. For such images, the procedure is robust and achieves similar precision to that of a manual technique, in which an operator chooses a set of points on the limbus.[28] The second image in Figure 3 was taken during the blink and corresponds to frame 11 of Figure 2. We note that the limbal extraction procedure as well as the instrument's own pupil extraction procedure may not necessarily provide reliable results in such cases. This is a typical problem in statistical image processing where only a small part of the elliptical outline is visible.[29] It can be overcome by using techniques in which the bias in the ellipse estimator is removed.[30] Alternatively, one may choose to use a more robust model for the limbal outline, such as a circle. Nevertheless, the topographical data during the blink need to be excluded from the analysis, so the basic least squares estimation of the elliptical limbal outline seems to be sufficient in our application. In cases where little information about the limbal outline is available in the videokeratoscopic image, using orthogonal least squares or fitting a circle to the data may be a more appropriate way to estimate the limbal displacements.

In Figure 4, we show examples of the displacements of the estimated centre of the corneal limbus from the videokeratoscopic axis, in the horizontal and vertical directions for a recording in which a subject was asked to blink and then to suppress blinking for a period of time. Circular and elliptic models were considered. The co-ordinates of the instrument's axis (estimated centre of the first ring) were extracted from the instrument's export data file. The data during the blink have been removed together with a three-frame buffer on each side of the blink. For clarity of the plots, we have sub-sampled the data at 10 Hz, while the original 50 Hz data is used in the analyses. It can be noted that the amplitudes of horizontal and vertical eye movements are different.

Sudden changes in limbal displacement may arise in the inter-blink interval due to loss of fixation and small eye movements. Note that for this particular recording the differences in the estimated position of the centres of a circular and an elliptical model are approximately 50 µm (approximately two pixels) in both horizontal and vertical directions. Also, the estimates of the limbal position are noisy because it is difficult to accurately define the limbal outline. This noise can be filtered by passing the displacement data through a low-pass digital filter.[31] Alternatively, one can estimate the trends to the displacement data. Rather than choosing a fixed order of the polynomial trend, we decided to estimate the order of the polynomial expansion by using an information criterion. This allows data to be adequately modelled in each inter-blink interval.

## Corneal wavefront

Another aspect of high-speed videokeratoscopic data analysis deals with corneal aberrations. Topographical data are often used to establish the corneal contribution to the optics of the eye. Corneal aberrations can be derived from the elevation data via raytracing.[4] These aberrations are normally calculated by

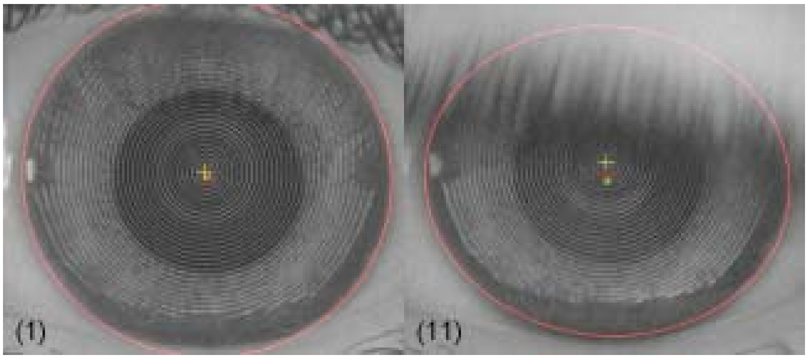

**Figure 3. Example of high speed videokeratoscopic images with estimated elliptical limbal outlines in the inter-blink interval (left) and during the blink (right). Yellow and red crosses denote the instrument axis, corresponding to the estimated centre of the first ring and the centre of the pupil, respectively. The green dots denote the centre of the estimated limbal outline.**

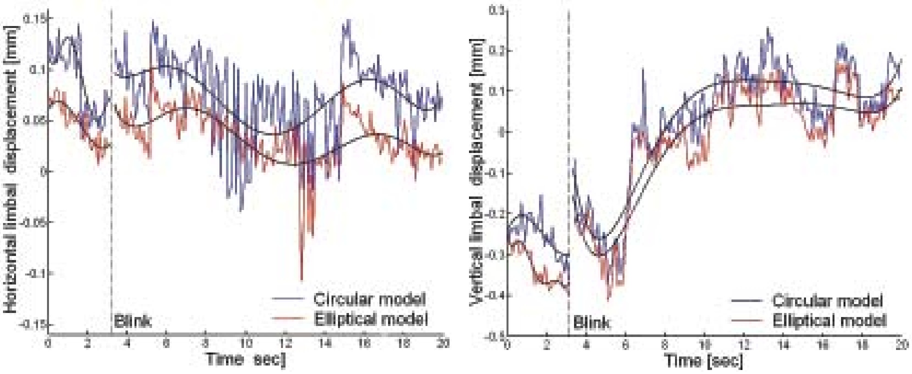

**Figure 4. Horizontal (left) and vertical (right) displacement of the estimated limbal centre with respect to the instrument's axis. The blue and red lines correspond to the circular and elliptical model of the limbal outline, respectively. Solid black lines show the estimated polynomial trends to the displacement data. The data in the plots are sub-sampled at 10 Hz for clarity of presentation.**

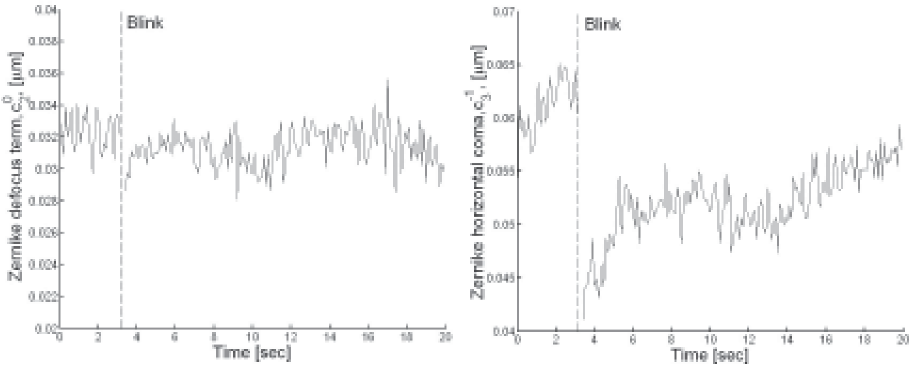

**Figure 5. Examples of dynamics in corneal aberrations. Defocus (left) and vertical coma (right) evaluated at 5 mm pupil diameter. The data in the plots are sub-sampled at 10 Hz for clarity of presentation.**

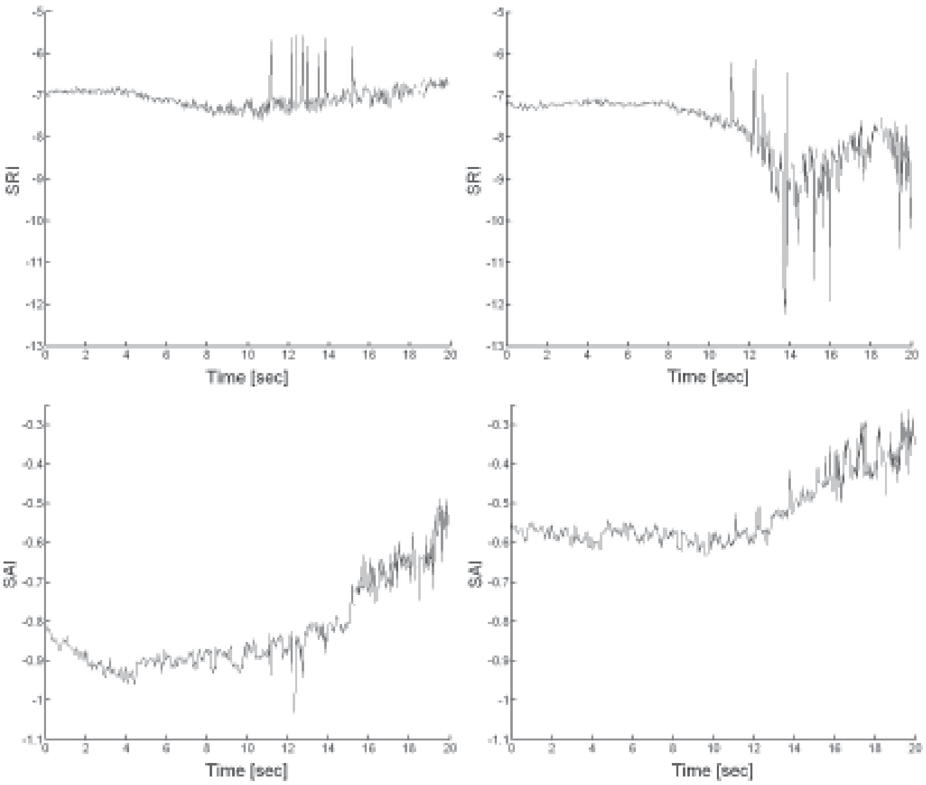

**Figure 6. Surface regularity (top) and asymmetry (bottom) indices for raw data (left) and the centred data (right) for a recording for a subject with corneal astigmatism and less stable tear film**

performing a 3D ray trace along the line-of-sight passing through the centre of the pupil. In such a case, knowledge of the limbal centre emphasised above may not be necessary. However, in this case, it is important to have good estimates of the pupillary centre. In addition, the relation between the pupillary and limbal centres is essential, if corneal aberrations are to be compared to the total aberration derived from a wavefront sensor,[10,32,33] for a pupil at a significantly different level of luminance (as the centre of the pupil may shift). Depending on the application, both limbal and pupillary centres may need to be estimated in high-speed videokeratoscopy. However, estimating the centre of the pupil in videokeratoscopy may be difficult, when the pupillary outline is covered by the reflection of the rings of the Placido disk or for subjects with dark irides.[34] Being aware of these limitations, we rely on the instrument's own estimator of the pupil centre.

In the continuous measurement of corneal aberrations, the estimated wavefront error can be fitted with a time-varying Zernike polynomial expansion[31]

$$W(\rho,\theta;t) = \sum_{n=0}^{N} \sum_{m=-M}^{M} c_n^m(t)\, Z_n^m(\rho,\theta)$$

where $m \leq n$, $n - |m| = even$, $(\rho,\theta)$ are the polar co-ordinates, with normalised to unity radial distance, $c_n^m(t)$ is the time-varying Zernike coefficient associated with $Z_n^m(\rho,\theta)$. The coefficients $c_n^m(t)$ can be estimated individually at discrete time instants $t_1, t_2, \ldots, t_T$ as in the case of a static measurement of wavefront aberration.

In Figure 5, we show examples of corneal aberrations (Zernike defocus, $c_0^2(t)$, and vertical coma, $c_3^{-1}(t)$, terms) for the same record that earlier we estimated the limbal displacement. Corneal aberrations were derived for a five-millimetre diameter pupil with the centre situated at the estimated centre of the pupil. The data for the pupillary centre were extracted from the instrument's export data file. For this particular record, we note that the defocus term is relatively constant, exhibiting only small variations in amplitude. In contrast, the vertical coma term has a distinct trend. Such a representation may be useful to determine the tear flow in the inter-blink interval.

In the following sections we will consider two specific applications of high-speed videokeratoscopy.

## TEAR FILM CHARACTERISATION

Traditionally, evaluation of tear film quality has been performed by applying fluorescein to the eye and observing the anterior corneal surface with a slitlamp. However, fluorescein instillation decreases tear film stability and may produce biased estimates of build-up and break-up times. Thus, non-invasive methods of tear film characterisation are preferred. There are several non-invasive techniques for tear film characterisation, such as meniscometry, interferometry, retro-illumination and wavefront sensing. In recent years, videokeratoscopy has also been used,[12,14-17] where observation of the tear film behaviour has focused on characterising SRI and SAI that are derived from maps of the estimated corneal power.[13] We use the following non-normalised surface regularity and asymmetry indices (without scaling constants, see Kojima and colleagues[16]) defined as

$$SRI = \ln\left[\frac{1}{N_M(N_R-2)} \times \sum_{i=1}^{N_M} \sum_{j=2}^{N_R-1} \left(P_{i,j} - 0.5\left[P_{i,j-1} + P_{i,j+1}\right]\right)\right]$$

and

$$SAI = \frac{2}{N_M N_R} \sum_{i=1}^{N_M/2} \sum_{j=1}^{N_R} \left(P_{i,j} - P_{i+N_M/2,j}\right)$$

where $N_M$ and $N_R$ are the number of considered meridians and rings in the data, respectively and $P_{i,j}$ is the value of power in dioptres at the $i$th meridian and $j$th ring.

For regular corneas, where there is little astigmatism or asymmetries in the cor-

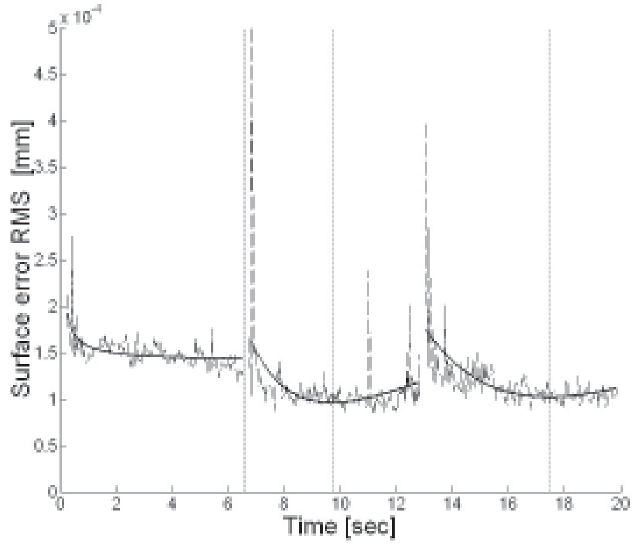

**Figure 7. An example of surface error RMS for a recording with three blinks. Solid thick lines indicate the estimated polynomial (in 1/t) trends. The vertical dashed lines indicate the positions at which the estimated trends achieve their minima.**

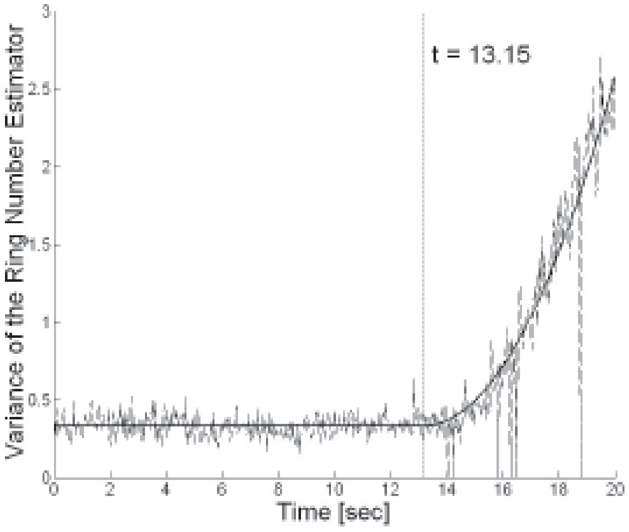

**Figure 8. The estimated variance of the ring number estimator for recording for a subject with corneal astigmatism and less stable tear film. The thick solid line shows functional estimation of the variance, while the vertical dotted line indicates the estimate of the tear-film break-up time.**

neal topography, centring the data to the common limbal reference for every frame of the videokeratograph may not be of great benefit. However, for less regular corneas, such as in astigmatism or keratoconus, the differences in SRI and SAI may be significant if this is not done. In Figure 6, we show results of SRI and SAI, where the difference between centring and not centring the data is evident. The results shown are for a record in which a subject with astigmatism and with less stable tear film suppressed blinking for the whole recording period of 20 seconds. In particular, we note that the SAI for raw data has a four-second period of decay followed by a 10-seond period of relative stability and a subsequent increase. This particular record was acquired a few seconds after the blink, so the initial decrease in the amplitude of the SAI cannot be attributed to the tear film build-up time.[12] After centring the data, the SAI is more stable and follows a 12-second period of relative stability before it increases. Visual inspection of the dynamic corneal topographic maps confirms this result.

To avoid ocular microfluctuations in the analysis of dynamic corneal data, there are two options. In the first, a common reference point to all dynamic data is to be found either by correlation techniques or by estimating the limbal centre as noted earlier. However, this is computationally intensive. Another way of avoiding the effects of ocular microfluctuations in the data is to use surface descriptors that are less dependent on the position of the instrument's axis.

In our recent work,[35] we used an approach that combined parametric modelling of corneal surfaces, statistics and image processing to estimate the tear film build-up and break-up times. The aim of parametric modelling is to decompose the measured corneal shape into a set of individual components. Such decompositions are essentially two-dimensional functions that are centred at some fixed point (origin), however like the SRI and SAI indices, they are also sensitive to the errors induced by ocular microfluctuations. To diminish their dependence on microfluctuations, we used the root mean square (RMS) of the residual surface error of the extracted elevation data and its estimated parametric model (for example, Zernike polynomial expansion[36]).

One of the main observations made when examining the behaviour of the residual surface error RMS was that centring corneal elevation data to a common reference point to remove the effect of microfluctuations did not significantly affect its magnitude. Analysing the behaviour of the surface error RMS suggested that it could be used for estimating tear film build-up time. Similarly, as in the case of modelling the displacement of the limbal centre, a trend function for the surface error RMS was suggested. In particular, a polynomial of second order in $1/t$ has been chosen, that is:

$$RMS(t) = \frac{at^2+bt+c}{t^2},\ t>0$$

where the parameters $a > 0$, $b < 0$ and $c > 0$ are estimated using a traditional least-square procedure. As this particular function follows a period of decay, reaches the minimum and then increases to the asymptotic value of $a$, it is important that it is used for full inter-blink records where

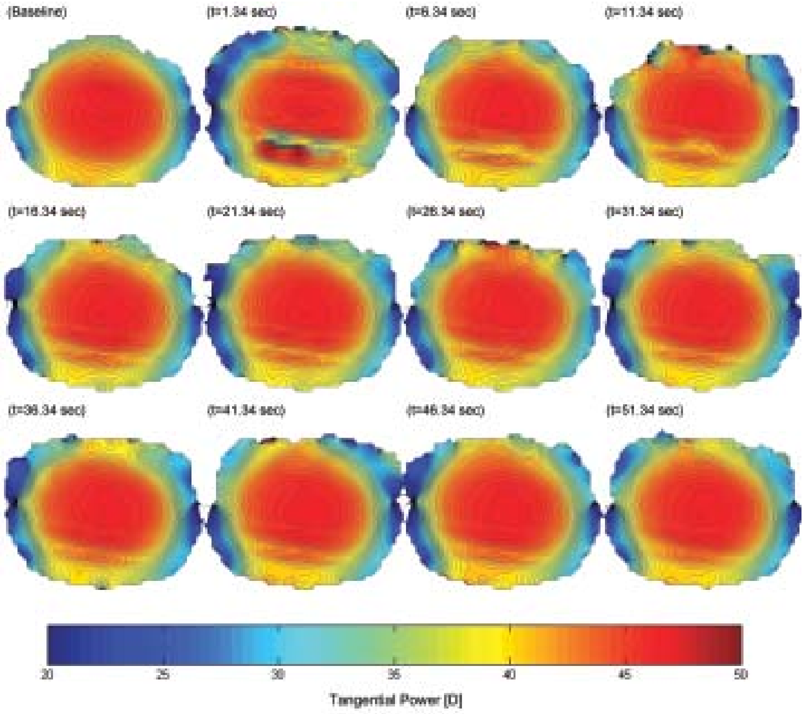

**Figure 9. Temporal changes in tangential power maps of a cornea after a one-minute eye movement task at a low gaze angle. The baseline tangential power map is an average topography from a one-minute baseline sequence recorded before the commencement of the task.**

the build-up of the tear film is occurring. The proposed model was found to be robust, having the ability to fit well for a variety of surface error RMS sequences. In Figure 7, we show an example of the surface error RMS for a recording with three blinks together with the estimated polynomial trends. The position at which each of the estimated trends achieves its minimum was also noted (vertical dashed lines in Figure 7). Eighth radial order Zernike polynomial expansion was used in this case.

The properties of the polynomial (in $1/t$) trend suggest that the location of its minimum should correspond to the time, at which the corneal surface (or the tear film) is sufficiently regular to be adequately modelled with a given Zernike polynomial expansion. This leads to a definition of the tear film build-up time as[35]

$$T_{BLD} = \underset{t}{\arg\min}\{RMS(t)\} - t_B$$

where $t_B$ is the time of the blink defined at the first topographically resolved videokeratoscopic image after a blink.

Unfortunately, the surface error RMS cannot be used to estimate accurately the tear film break-up time. There are several reasons for this. First, it is difficult to place an arbitrary threshold on the amplitude of the surface error RMS, at which the tear film is supposedly breaking up. Second, the polynomial trend chosen to model the build-up and relatively stable phases increases asymptotically to a bounded value of the parameter. Finally, videokeratoscopic routines for estimating corneal surfaces rely heavily on the quality of the acquired images, which significantly degrade during the break-up of the tear film. Taking into account the definition of tear film break-up time,[37] it becomes clear that it is essential to use the original ring pattern images for the task of estimating tear film break-up time.

Recently, we have proposed a simple yet effective method for this task.[35] In essence, the method estimates the variance of the number of rings detected radially from the centre of the videokeratoscopic image. The changes in this variance indicate the instability in image quality that is directly related to the quality of the tear film. An example of the estimated variance of the number of rings for the previously considered recording of a subject with astigmatism and less stable tear film is shown in Figure 8. We note that when the eye is kept open for a sufficiently long period, the ring number variance has two distinct regions. The first region is relatively constant while the second region after a period can be estimated by a quadratic function. The transition from the linear trend to the quadratic trend has been used as an estimator of the tear-film break-up time.[35]

## DYNAMICS OF CORNEAL BIOMECHANICS

The corneal surface can be altered with mechanical forces such as those from natural lid pressure[19,20] or a contact lens.[21,38] The changes in the corneal surface are often small and the regression is normally fast. In some cases, such as reading, lid induced forces may result in substantial changes in corneal elevation, which significantly change the optical properties of the eye.[39] These changes are more persistent and recovery of corneal surface may take minutes or hours.[22]

Modelling of the stress-strain response of the corneal surface is possible *in vitro*[40] but is difficult for real corneas *in vivo*. High speed videokeratoscopy provides the means to quantify the dynamic changes in the corneal surface that may occur during and after a mechanical force is applied to the cornea. The resulting dynamic topographical data can be utilised for biomechanical modelling of the corneal surface.

To illustrate this application of high speed videokeratoscopy, we performed an experiment in which a subject was positioned in the instrument head rest and a sequence of baseline dynamic topographs was recorded over one minute. Still positioned in the head rest, the subject was asked to perform horizontal eye movements by alternating fixation (with the fellow eye) between two cross targets about 45 degrees below horizontal and separated by a visual angle of about 30 degrees for a period of one minute. Immediately after the eye movement task, the subject was asked to look at the instrument's internal fixation target and a sequence of dynamic topographical data was again recorded for a period of one minute. The subject was instructed to blink naturally throughout the experiment.

In Figure 9, we show temporal changes (every five seconds) in the tangential power maps for the subject after the one-minute eye movement task in downward gaze. The baseline tangential power map, shown in the left top corner of Figure 10, shows an average topography derived from a one-minute baseline sequence recorded before the commencement of the eye movement task. Blinks together with three-frame samples on each side of the blink have not been included in the average. In the first second of the recording, the subject was still changing gaze position (from downward gaze to the instrument axis) and performed several blinks. Thus, the first topographically resolved image of the recording (frame 68) corresponds to $t$ = 1.34 sec. The results indicate that a simple exercise such as horizontal eye movements in downward gaze can result in significant changes to the corneal surface. In Figure 10, we show the raw videokeratoscopic images corresponding to the beginning and the end phases of this recording, together with residual height maps taken from the estimated best aspheric surface. The effect of the force exerted by the lower eyelid margin on the inferior cornea is clearly visible in these images. As its position is within the area of the pupil, significant optical changes are also expected. We also note that the lower lid force causes both vertical and horizontal changes in corneal elevation, having the greatest effect in the inferior central region of the map.

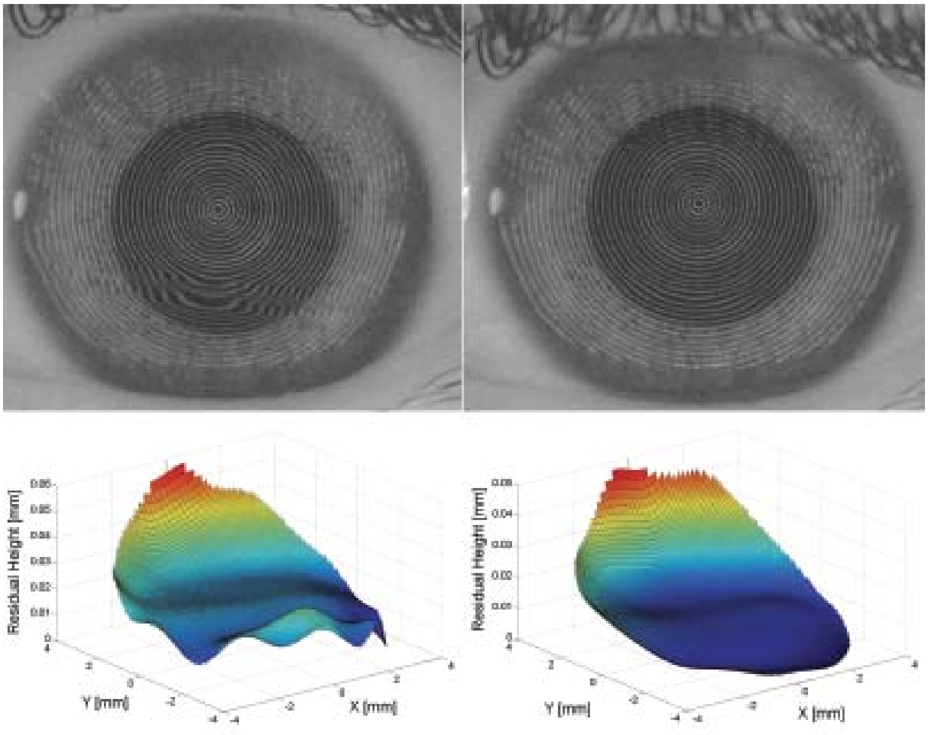

**Figure 10. Raw videokeratoscopic images at the beginning (left) and end (right) of the recording after a one-minute eye movement task at a low gaze angle and the corresponding residual heights taken from the estimated best aspheric surface.**

Measurement of temporal changes in corneal topography and subsequent analysis of these corneal dynamics provide the means to study the biomechanics of the cornea *in vivo*. However, the extreme changes in corneal curvature, such as the one at the beginning of the considered sequence of measurements (Figure 10), have to be viewed with caution when utilising traditional videokeratoscopes because they may not be designed to adequately process data from such distorted surfaces.[26]

## CONCLUSIONS

High-speed videokeratoscopy opens new opportunities for studies of the anterior eye, such as characterisation of tear film dynamics and the analysis of corneal biomechanics. Other potential applications include subjects who are unable to focus on the instrument's target or have uncontrolled eye movements. Examples of this application of the technology would be subjects with nystagmus, infants or animal research. By examining the sequence of continuously acquired videokeratographic images, the user could choose the map, which shows the most appropriate alignment of the instrument axis and cornea.

As with any technology, high-speed videokeratoscopy has limitations. Most current videokeratoscopes are based on imaging a fixed faceplate, such as the Placido rings cone, for which high-speed acquisition can be adapted easily. However, this would not be practical in videokeratoscopes based on the slit scanning method because of the time required to construct a single map. Achieving dynamic acquisition of corneal topographical data requires much higher sampling rates and the ability to move the scanning slit at a much faster rate.

There are also general hardware limitations of high speed videokeratoscopy that include sampling frequency, ability to acquire data in real time without jitter and the size of available computer memory (regarding both dynamic acquisition and storage). As computer technology is growing at an almost exponential rate, it is likely that the technology of high speed videokeratoscopy will not be limited by computer hardware in the future.

## ACKNOWLEDGEMENTS

We thank Brett Davis, Tobias Buehren, Stephanie Voetz and Alyra Shaw for their help in different aspects of the clinical experiments. Special thanks to Grant Frisken for writing the DV2000/E300 image converter.

## GRANTS AND FINANCIAL SUPPORT

This project was supported by the QUT Strategic Collaborative Program scheme.

## COMMERCIAL INTERESTS

None of the authors has a financial interest in any product mentioned.

## REFERENCES:

1. Mandell RB. A guide to videokeratography. *Int Contact Lens Clin* 1996; 23: 205–228.
2. Schwiegerling J, Greivenkamp JE. Keratoconus detection based on videokeratoscopic height data. *Optom Vis Sci* 1996; 73: 721-728.
3. Szczotka LB, Roberts C, Herderick EE, Mahmoud A. Quantitative descriptors of corneal topography that influence soft toric contact lens fitting. *Cornea* 2002; 21: 249-255.
4. Guirao A, Artal P. Corneal wave aberration from videokeratography: accuracy and limitations of the procedure. *J Opt Soc Am A* 2000; 17: 955-965.
5. TMS-2N Corneal Topographer. Tomey Corporation, Nagoya, Japan.
6. E300 Corneal Topographer. Medmont, Melbourne, Australia.
7. Tsubota K. Tear dynamics and dry eye. *Prog Ret Eye Res* 1998; 17: 556-596.
8. Buehren T, Collins MJ, Iskander DR, Davis B, Lingelbach B. The stability of corneal topography in the post-blink interval. *Cornea* 2001; 20: 826-833.
9. Nemeth J, Erdelyi B, Csakany B. Corneal topography changes after a 15 second pause in blinking. *J Cataract Refract Surg* 2001; 27: 589-592.
10. Montés-Micó R, Alió JL, Muñoz G, Pérez-Santonja JJ, Charman WN. Postblink changes in total and corneal ocular aberrations. *Ophthalmology* 2004; 111: 758-767.
11. Montés-Micó R, Alió JL, Muñoz G, Charman WN. Temporal changes in optical quality of air-tear film interface at anterior cornea after blink. *Invest Ophthalmol Vis Sci* 2004; 45: 1752-1757.
12. Nemeth J, Erdelyi B, Csakany B, Gaspar P, Soumelidis A, Kahlesh F, Lang Z. High-speed videokeratoscopy measurement of tear film build-up time. *Invest Ophthalmol Vis Sci* 2002; 43: 1783-1790.
13. Dingeldein SA, Klyce SD, Wilson SE. Quantitative descriptors of corneal shape derived from computer-assisted analysis of photokeratographs. *J Refrat Corneal Surg* 1989; 5: 372-378.
14. Goto T, Zheng X, Klyce SD, Kataoka H, Uno T, Karon M, Tatematsu Y, Bessyo T, Tsubota K, Ohashi Y. A new method for tear film stability analysis using videokeratoscopy. *Am J Ophthalmol* 2003; 135: 608-612.
15. Goto T, Zheng X, Klyce SD, Kataoka H, Uno T, Yamaguchi M, Karon M, Hirano S, Okamoto S, Ohashi, Y. Evaluation of the tear film stability after laser *in situ* keratomileusis using tear film stability system. *Am J Ophthalmol* 2004; 137: 116-120.
16. Kojima T, Ishida R, Dogru M, Goto E, Takano Y, Matsumoto Y, Kaido M, Ohashi Y, Tsubota K. A new noninvasive tear stability analysis system for assessment of dry eyes. *Invest Ophthalmol Vis Sci* 2004; 45: 1369-1374.
17. Goto T, Zheng X, Okamoto S, Ohashi Y. Tear film stability analysis system. *Cornea* 2004; 23: S65-S70.
18. Grey C, Yap M. Influence of lid position on astigmatism. *Am J Optom Physiol Opt* 1986; 63: 966-969.
19. Lieberman DM, Grierson JW. The lids influence on corneal shape. *Cornea* 2000; 19: 336-342.
20. Buehren T, Collins MJ, Carney L. Corneal aberrations and reading. *Optom Vis Sci* 2003; 80: 159-166.
21. Voetz SC, Collins MJ, Lingelbach B. Recovery of corneal topography and vision following opaque-tinted contact lens wear. *Eye Contact Lens* 2004; 30:111-117.
22. Collins MJ, Kloevekorn-Norgall K, Buehren T, Voetz SC, Lingelbach B. Regression of lid-induced corneal topography changes following reading. *Optom Vis Sci* 2005. In press.
23. Buehren T, Lee BJ, Collins MJ, Iskander DR. Ocular microfluctuations in videokeratoscopy. *Cornea* 2002; 21: 346-351.
24. Greivenkamp JE, Mellinger MD, Snyder RW, Schwiegerling JT, Lowman AE, Miller JM. Comparison of three videokeratoscopes in measurement of toric test surfaces. *J Refract Surg* 1996; 12: 229-239.
25. Schultze RL. Accuracy of corneal elevation with four corneal topography systems. *J Refract Surg* 1998; 14: 100-104.
26. Tang W, Collins MJ, Carney L, Davis B. The accuracy and precision performance of four videokeratoscopes in measuring test surfaces. *Optom Vis Sci* 2000; 77: 483-491.
27. Franklin R, Morelande MR, Iskander DR, Collins MJ, Davis BA. Combining central and peripheral videokeratoscope maps to investigate total corneal topography. *Eye Cont Lens* 2005. In press.
28. Morelande MR, Iskander DR, Collins MJ, Franklin R. Automatic estimation of the corneal limbus in videokeratoscopy. *IEEE Trans Biomed Eng* 2002; 49: 1617-1625.
29. Rosin PL. A note on least squares fitting of ellipses. *Pattern Recognition Letters* 1993; 14: 799-808.
30. Cabrera J, Meer P. Unbiased estimation of ellipses by bootstrapping. *IEEE Trans Pattern Analysis Machine Intell* 1996; 18: 752-756.
31. Iskander DR, Collins MJ, Morelande MR, Zhu M. Analyzing the dynamic wavefront aberrations in human eye. *IEEE Trans Biomed Eng* 2004; 51: 1969-1980.
32. Marcos S, Barbero S, Llorente L, Merayo-Lloves J. Optical response to LASIK surgery for myopia from total and corneal aberration measurements. *Invest Ophthalmol Vis Sci* 2001; 42: 3349-3356.
33. Mrochen M, Jankov M, Bueeler M, Seiler T. Correlation between corneal and total wavefront aberrations in myopic eyes. *J Refract Surg* 2003; 19: 104-112.
34. Fogla R, Rao SK. Pupillometry using videokeratography in eyes with dark brown irides. *J Cataract Refract Surg* 2000; 26: 1266-1267.
35. Iskander DR, Collins MJ, Davis B. Evaluating tear film stability in the human eye with high speed videokeratoscopy. *IEEE Trans Biomed Eng*. In press.
36. Schwiegerling J, Greivenkamp JE, Miller JM. Representation of videokeratoscopic height data with Zernike polynomials. *J Opt Soc Am A* 1995; 12: 2105-2113.
37. Mengher LS, Bron AJ, Tonge SR, Gilbert DJ. A non-invasive instrument for the clinical assessment of the pre-corneal tear film stability. *Curr Eye Res* 1985; 4: 1-7.
38. Moezzi AM, Fonn D, Simpson TL, Sorbara L. Contact lens-induced corneal swelling and surface changes measured with the Orbscan II corneal topographer. *Optom Vis Sci* 2004; 81: 189-193.
39. Buehren T, Collins MJ, Carney LG. Near work induced wavefront aberrations in myopia. *Vision Res* 2005; 45: 1297-1312.
40. Hjortdal, JØ. Regional elastic performance of the human cornea. *J Biomech* 1996; 29: 931-942.

Corresponding author:
D Robert Iskander
Contact Lens and Visual Optics
Laboratory
School of Optometry
Queensland University of Technology
Victoria Park Road
Kelvin Grove QLD 4059
AUSTRALIA
d.iskander@qut.edu.au